

# Microscopic Theory of Magnetic Phase Transitions in $\text{HoNi}_2\text{B}_2\text{C}$

A. Amici<sup>1</sup> and P. Thalmeier<sup>2</sup>

<sup>1</sup>*Max-Planck-Institut für Physik komplexer Systeme, 01187 Dresden Germany,*

<sup>2</sup>*Max-Planck-Institut für chemische Physik fester Stoffe, 01187 Dresden, Germany*

(September 13, 2018)

## Abstract

We present a microscopic theory for the low temperature metamagnetic phase diagram of  $\text{HoNi}_2\text{B}_2\text{C}$  that agrees well with experiments. For the same model we determined the zero field ground state as a function of temperature and find the  $c$ -axis commensurate to incommensurate transition in the expected temperature range. The complex behaviour of the system originates from the competition between the crystalline electric field and the Ruderman-Kittel-Kasuya-Yosida interaction, whose effective form is obtained. No essential influence of superconductivity has to be invoked to understand the magnetic phase diagram of this material.

The recent interest in  $\text{HoNi}_2\text{B}_2\text{C}$  and similar borocarbide compounds is motivated by the possibility of a detailed study of the mutual interaction between superconductivity (SC) [1] and magnetic order (MO) [2,3] coexisting in a few of these materials as bulk properties. The superconducting critical temperature for  $\text{HoNi}_2\text{B}_2\text{C}$  is  $T_c = 8$  K [1] and the upper critical field  $H_{c2}^{sc}$  is about  $2 \sim 3.5$  kG [4]. Temperature dependent measurements show a pronounced anomaly of  $H_{c2}^{sc}(T)$  around 5 K which nearly leads the material to reentrance into the normal state [2,5]. In the same temperature range several magnetically ordered structures are observed in the Ho f-electrons sub-lattice: a commensurate (C) antiferromagnetic phase below 5 K [2,3], an incommensurate (IC) *c*-axis complex spiral state ( $5 \text{ K} < T < 6 \text{ K}$ ) [3,6,7] and an *a*-axis IC modulation in a narrow range of temperature around 5.5 K [6,8]. Although no satisfactory theory is available presently, many experiments point to a correlation between this complex magnetic phase diagram and the SC anomalies [9,10]. Much insight on the magnetism of this material can be gained from a number of experiments reporting metamagnetic transitions at low temperature and fields higher than  $H_{c2}^{sc}$  [2,11]. In particular the detailed anisotropic metamagnetic phase diagram at  $T = 2$  K presented in Ref. [12], can be used to extract many features of the magnetic interaction. In this work we propose a realistic microscopic model for the Ho 4*f*-electrons sub-system of  $\text{HoNi}_2\text{B}_2\text{C}$  which reproduces the main features of the low temperature metamagnetic phase diagram as well as the zero field sequence of phases as function of temperature. It is important to note that many physical elements need to be included in the present theoretical description to have reasonable agreement with experiments and likely a model of a comparable complexity is needed to treat the mutual interaction between SC and MO.

The coexistence and weak coupling of the two phenomena of SC and MO is due to the different degrees of localisation of electrons in the borocarbides. LDA calculations show that the conduction band is composed mainly of Ni 3*d*-electrons [13], which undergo the superconducting transition. On the other hand magnetic properties are related to the well localised electrons in the incomplete 4*f*-shell of Ho. The exchange interaction between these two electron systems is mediated by the small fraction of Ho 6*s* and 5*d* character in the

conduction band. As far as magnetic properties are concerned the conduction electrons can be eliminated in a standard way leading to an effective RKKY exchange interaction among the stable Ho  $4f$  moments. The appropriate Hamiltonian is then given by [14]:

$$\mathcal{H} = \sum_i [\mathcal{H}_{cf}(\mathbf{J}_i) - \boldsymbol{\mu}_i \cdot \mathbf{B}] - \frac{1}{2} \sum_{ij} \mathcal{J}(i, j) \mathbf{J}_i \cdot \mathbf{J}_j \quad (1)$$

This Hamiltonian include the crystal electric field (CEF) single ion part  $\mathcal{H}_{cf}(\mathbf{J}_i)$  expressed in terms of the total angular momentum  $\mathbf{J}_i$ , the Zeeman interaction between the local magnetic induction  $\mathbf{B}$  and the magnetic moment  $\boldsymbol{\mu}_i = \mu_B g \mathbf{J}_i$  ( $\mu_B$  is the Bohr magneton and  $g = \frac{5}{4}$  the gyromagnetic ratio for Ho), and the effective RKKY exchange interaction. The direct dipole-dipole interaction is not relevant in borocarbides [15] and this allows us to use a magnetic induction field  $\mathbf{B}$  independent of the position. The CEF single ion Hamiltonian we use is the one extracted from neutron diffraction experiments in Ref. [16] and contains no adjustable parameter. Its ground state is a  $\Gamma_4$  singlet and the first exited states are a  $\Gamma_5^*$  doublet at 0.15 meV from the ground state and a  $\Gamma_1$  singlet at 0.32 meV. The other 13 CEF states have much higher excitation energies ( $> 10$  meV) and their matrix elements with the low energy quartet is very small, therefore they may be neglected in the whole range of temperature and fields which we explored. Regarding the magnetic interaction no previous knowledge is available about the RKKY function  $\mathcal{J}(i, j)$  and an important aim of this work is to obtain a realistic model for it.

Since we are dealing with a three dimensional system of large angular momenta ( $J_{Ho} = 8$ ) it is possible to treat its Hamiltonian at a mean field (MF) level. Introducing the mean thermal value  $\langle \mathbf{J}_i \rangle$  and neglecting the terms containing two sites fluctuations it is possible to decouple the dynamics of the different sites. The single ion MF Hamiltonian is then given by [14]:

$$\mathcal{H}_{mf}(i) = \mathcal{H}_{cf}(\mathbf{J}_i) - \mathbf{J}_i \cdot \mathbf{B}_i^e + \mathcal{E} \quad (2)$$

in which  $\mathbf{B}_i^e = (\mu_B g \mathbf{B} + \sum_j \mathcal{J}(i, j) \langle \mathbf{J}_j \rangle)$  is the effective molecular field and  $\mathcal{E} = \frac{1}{2} \langle \mathbf{J}_i \rangle \sum_j \mathcal{J}(i, j) \langle \mathbf{J}_j \rangle$ . The diagonalisation of this single site Hamiltonian can be easily

achieved numerically. The single ion Gibbs free energy density  $F_i^M$  and the corresponding average angular momentum  $\langle \mathbf{J}_i \rangle$  can be computed as functions of  $\mathbf{B}_i^e$  and  $T$ . This leads to the self consistent MF equations for the  $\langle \mathbf{J}_i \rangle$  which can be solved iteratively. Two experimental evidences can be used to reduce the number of independent sites whose MF magnetisation should be computed. First of all, almost all the observed structures in this compound share the property of ferromagnetic alignment in the  $ab$  plane. The only exception is the  $a$ -axis modulation whose structure is not yet clear. However it appears not to coexist microscopically with the  $c$ -axis ones [7] and we will neglect it. Therefore we impose ferromagnetic alignment in the plane from the beginning thus reducing the calculation to one dimension. Then the RKKY interaction have only  $c$ -dependence and, taking the magnetic moment in the site 0 as the reference, it may be parametrised with the help of  $\mathcal{J}_i = \sum_{\{j_i\}} \mathcal{J}(0, j_i)$ , with  $j_i$  running on all the sites of the  $i^{th}$  plane. The  $\mathcal{J}_i$  with  $i \geq 1$  are the interaction of the reference moment with those in the neighbouring layers and  $\mathcal{J}_0$  is the interaction with the other moments in the same plane. The second simplification is related to the CEF structure, in fact the  $c$ -axis is a very hard direction in the whole range of temperature we are interested in, therefore we force the moments to lie in the  $ab$  plane neglecting their small out-of-plane component.

In order to establish the actual MF ground configuration for the  $\langle \mathbf{J}_i \rangle$  out of the possible stable ones we introduce the Helmholtz free energy (HFE) density given by:

$$F(\mathbf{r}) = F^M(\mathbf{B}) + \frac{B^2}{8\pi} - \frac{\mathbf{H} \cdot \mathbf{B}}{4\pi} = F^M(\mathbf{B}) - 2\pi M^2 - \frac{H^2}{8\pi} \quad (3)$$

with  $\mathbf{B}(\mathbf{r}) = \mathbf{H}(\mathbf{r}) + 4\pi\mathbf{M}(\mathbf{r})$  [17]. The integral of  $F(\mathbf{r})$  over all space is the proper thermodynamic function to be minimised when external fields are kept constant [17]. The magnetisation contribution ( $\sim 10$  kG) is not negligible with respect to the typical external field (4-25 kG). However the full problem of solving for  $\mathbf{M}(\mathbf{r})$  in a finite sample with a given geometry is beyond our purpose. This is indeed a typical problem in thermodynamics of magnetic materials [17] whose most practical solution is to assume cylindrical symmetry around the external field  $\mathbf{H}$  in order to eliminate the spatial dependence of both  $\mathbf{B}$  and  $\mathbf{M}$ .

The homogeneous magnetisation of the sample is calculated as  $\mathbf{M} = \frac{g\mu_B}{V_c} \overline{\langle \mathbf{J}_i \rangle}$  where  $V_c = 65 \text{ \AA}^3$  is the volume of the unit cell and the bar indicates the average on all ions. Similarly the contribution of the magnetisation to the HFE per unit cell can be written as  $2\pi M^2 V = \frac{2\pi(g\mu_B)^2}{V_c} \overline{\langle \mathbf{J}_i \rangle^2}$ .

Until now the actual RKKY interaction among magnetic moments remained unspecified. In order to achieve a convenient parametrisation for it we make an extensive use of the  $T = 2\text{K}$  magnetisation data in Ref. [12]. From the clear presence of flat magnetisation plateaux and from the value of the magnetisation as a function of the angle we argue that the magnetic moments of the ions are almost at the saturation value  $J_s = J_{Ho} = 8$  and they are locked in one of the four equivalent  $\langle 110 \rangle$  in-plane easy directions [12]. The sharp metamagnetic transitions are then due to first order transitions among different arrangement of the moments along the  $c$ -axis. We assume that the relevant phases in the field-angle phase diagram are the easiest commensurate structures with the observed magnetisation (they are listed in the upper part of table I). We notice that all the phases in table I may be represented in a chain of six unit cells with periodic boundary conditions. This is important because the Fourier transform of the interaction for a system with six sites have only four free parameter, namely  $\mathcal{J}_i$  with  $i = 0, 1, 2, 3$ . Any further Fourier component may be removed with a renormalisation of these parameters (i.e. the  $\mathcal{J}_6$  is equivalent to  $\mathcal{J}_0$ ). Neglecting the CEF energy and entropy it is possible to calculate analytically the HFE for each configuration. Some of these energies are listed in table I. From the two  $\theta = 0^\circ$  metamagnetic transitions it is possible to establish two conditions for the parametrisation of the RKKY interaction. Following the convention of Canfield *et. al.* [12] we call the metamagnetic transition fields  $H_{c1} = 4.1 \text{ kG}$  and  $H_{c2} = 11.1 \text{ kG}$  (this value is somewhat higher than the  $10.6 \text{ kG}$  given in Ref. [12]), they should not be confused with the superconducting critical fields. Imposing the energy of the AF2 and AF3 phases to be equal at  $H_{c1}$  and the ones of AF3 and P at  $H_{c2}$  we obtain the following relations:

$$\mathcal{J}_1 = -\mathcal{J}_2 - \frac{g\mu_B}{2J_s} H_{c2} - \frac{2}{3} E_M \quad (4)$$

$$\mathcal{J}_3 = \mathcal{J}_2 + \frac{g\mu_B}{6J_s}(H_{c2} - H_{c1}) + \frac{1}{6}E_M$$

where  $E_M = \frac{2\pi(g\mu_B)^2}{V_c} = 8.1 \cdot 10^{-3}$  meV comes from the contribution of the magnetisation to the HFE. They assure that the relative stability of the three phases for  $\theta = 0^\circ$  is the observed one. In order to use the easiest possible model we set  $\mathcal{J}_3 = 0$ , which implies  $\mathcal{J}_1 = -8.0 \cdot 10^{-3}$  meV and  $\mathcal{J}_2 = -2.4 \cdot 10^{-3}$  meV. The final freedom in the model is the parameter  $\mathcal{J}_0$  which works basically as a self interaction and cannot be extracted starting from the energy differences among magnetic structures. We use  $\mathcal{J}_0 = 4.8 \cdot 10^{-3}$  meV in order to have the transition between the paramagnetic and the incommensurate state at the experimental value  $T = 6$  K [4]. Moreover this choice make the internal molecular field large enough ( $\sim 15$  kG) to maintain the moments close to the saturation regime, as required.

After the model has been defined and all its parameters fixed we present now the numerical results of the complete self consistent MF calculation for the field-angle phase diagram at  $T = 2$  K. The starting values for  $\langle \mathbf{J}_i \rangle$  in the iteration algorithm are a set of random numbers and the possible periods allowed are in the range from one to nineteen planes. Typical magnetisation curves are evaluated and they are shown in fig. 1, they refer to experimental geometries with different angles  $\theta$  between the external field  $\mathbf{H}$  and the closest magnetic easy axis  $\langle 110 \rangle$ . The resulting metamagnetic phase diagram is presented in fig. 2. It contains all the phases in the table I and it agrees remarkably well with the experimental one. In particular all the transition lines show simple trigonometrical dependence as a function of the angle  $\theta$  as well as the corresponding magnetisation values at the plateaux. In all the regions where the stable phases are AF2, AF3, F3 and P we observe remarkable quantitative agreement with the experimental data in Ref. [12]. The main qualitative differences between our model and experiments is the presence of two additional phases, the F2 and the C6, whose magnetisation is different from the reported ones. However the strongest disagreement is in the region of relatively low field and high angles where experimentally the strongest hysteresis is found. Another minor point is the absence of direct AF3-P transition for  $\theta \neq 0^\circ$ . Experimentally the direct transition is observed for small angles up to  $\theta = 6^\circ$  in

the Ho compounds, but seems to have a much wider range in the similar phase diagram of  $\text{DyNi}_2\text{B}_2\text{C}$  [18]. We would like to stress however that it is not possible to improve this phase diagram simply refining the parameters for the RKKY interaction. For example allowing for  $\mathcal{J}_3 \neq 0$  it is possible to stabilise at low field an additional phase, which is a distorted helix structure with wave length five, but no change appears in the phase transitions among the other phases. In addition, as explained before, the effect of further effective interactions with neighbouring planes beyond the third one may be eliminated by proper renormalisation of the  $\mathcal{J}_i$  with  $i < 3$ . Therefore if the two phases F2 and C6 are not observed in the experiments we have to conclude that additional interactions (i.e. magnetoelastic couplings) have to play a role in the stability of magnetic phases in  $\text{HoNi}_2\text{B}_2\text{C}$ .

Starting from the same model it is possible to analyse the zero field behaviour as a function of temperature. In principle this requires some attention since the magnetic system is now embedded in a superconducting material. This implies important changes in the  $\mathbf{q} \sim 0$  region of the Fourier transform of the RKKY function [19], but leaves the relevant  $\mathbf{q} \sim \pi$  region almost unchanged. Relying on this fact and on experiments on doped non-superconducting materials such as  $\text{HoNi}_{2-x}\text{Co}_x\text{B}_2\text{C}$  which show a magnetic behaviour very similar to the undoped superconducting one [20,21], we will use our purely magnetic model for the description of the zero field phase diagram. At MF level the second order phase transition between the paramagnetic state and an ordered structure is expected to occur at the  $\mathbf{Q}$  vector for which the  $\mathcal{J}(\mathbf{q})$  has its maximum. In our model this correspond to  $\mathbf{Q}_c = 0.78\pi$  in the  $\langle 001 \rangle$  direction, not far from the experimental value  $\mathbf{Q}_{exp} = 0.91\pi$  [7]. The helical state is preferred with respect to the longitudinal modulated structure due to the *ab* easy plane for the moments. This truly incommensurate structure can be the ground state of the system only as long as the average moment per ion is small enough, i.e. close to the transition temperature. Lowering the temperature the ordered state develops and the CEF part of the HFE, proportional to fourth and the sixth powers in  $\langle \mathbf{J}_i \rangle$ , force the structure to find a commensurate compromise. Because in the self consistent MF treatment it is not possible to treat at the same time truly incommensurate structures and the CEF, we cannot

observe the actual C-IC transition. However at a temperature of  $T = 5.5$  K is observed a first order transition from AF2 to a helical state of wave length 17, where the moments point no longer only along the easy directions. This is the clear indication that the RKKY energy starts to become dominant with respect to the CEF potential and drives the system into a state whose wave number  $\mathbf{Q}$  is closer to the maximum of the RKKY function. To obtain better quantitative agreement for the ordering wave number *and* for the temperature interval in which the incommensurate state is stable, the function  $\mathcal{J}(\mathbf{q})$  has to be refined in the  $\mathbf{Q}_c$  region by including further parameters.

In conclusion, we presented a microscopic model for the the rare earth borocarbide system  $\text{HoNi}_2\text{B}_2\text{C}$  which explains the main reported features of the anisotropic magnetic and temperature phase diagrams. The minimal model to achieve a semiquantitative description of the complex magnetic behaviour of the system needs to include realistic CEF and effective RKKY interaction among the planes. On the other hand no influence of SC needs to be included in the determination of the magnetic structures observed.

We would like to thank W. Henggeler *et al.* for the data on the CEF states. A.A. would also like to thank M. Laad, P. De Los Rios and B. Canals. This work was performed under DFG Sonderforschungsbereich 463.

## REFERENCES

- [1] R. J. Cava *et al.*, *Nature* **367**, 252 (1994)
- [2] P. C. Canfield *et al.*, *Physica C* **230**, 397 (1994)
- [3] T. E. Grigereit *et al.*, *Phys. Rev. Lett.* **73**, 2756 (1994)
- [4] M. S. Lin *et al.*, *Phys. Rev. B* **52**, 1181 (1995)
- [5] R. J. Eisaki *et al.*, *Phys. Rev. B* **50**, 647 (1994)
- [6] A. I. Goldman *et al.*, *Phys. Rev. B* **50**, 9668 (1994)
- [7] J. P. Hill *et al.*, *Phys. Rev. B* **53**, 3487 (1996)
- [8] Comment to Ref. [3] by T. Vogt *et al.*, *Phys. Rev. Lett.* **75**, 2628 (1995) and the Reply by T. E. Grigereit *et al.*, *Phys. Rev. Lett.* **75**, 2629 (1995)
- [9] K. D. D. Rathnayaka *et al.*, *Phys. Rev. B* **53**, 5688 (1996)
- [10] H. Schmidt and H. F. Braun, *Phys. Rev. B* **55**, 8497 (1997)
- [11] B. K. Cho *et al.*, *Phys. Rev. B* **53**, 2217 (1996)
- [12] P. C. Canfield *et al.*, *Phys. Rev. B* **55**, 970 (1997)
- [13] L. F. Mattheiss, *Phys. Rev. B* **48**, 13279 (1994)
- [14] J. Jensen and A. R. Mackintosh, 'Rare Earth Magnetism', Oxford Science Publications (1991)
- [15] M. L. Kulić, A. I. Buzdin and L. N. Bulaevskii, cond-mat/9707024 (unpublished)
- [16] U. Gasser *et al.*, *Z. Phys. B* **101**, 345 (1996)
- [17] L. D. Landau, E. M. Lifshitz and L. P. Pitaevskii, 'Electrodynamics of Continuous Media', Butterworth-Heinemann (1984)
- [18] P. C. Canfield *et al.*, *Physica C* (to be published)

[19] P. W. Anderson and H. Suhl, Phys. Rev. **116**, 898 (1959)

[20] J. W. Lynn *et al.*, Phys. Rev. B **53**, 802 (1996)

[21] P. Allenspach *et al.*, Physica B **230-232**, 882 (1997)

TABLES

Phase	Structure	HFE per site
P	$\nwarrow$	$-J_s^2(\mathcal{J}_1 + \mathcal{J}_2 + \mathcal{J}_3 + E_M) - J_s H_{\parallel}$
AF2	$\nwarrow \searrow$	$J_s^2(\mathcal{J}_1 - \mathcal{J}_2 + \mathcal{J}_3)$
AF2'	$\nearrow \nwarrow$	$J_s^2(\mathcal{J}_1 - \mathcal{J}_2 + \mathcal{J}_3)$
AF3	$\nwarrow \searrow \nearrow$	$[J_s^2(\mathcal{J}_1 + \mathcal{J}_2 - 3\mathcal{J}_3 - E_M/3) - J_s H_{\parallel}]/3$
AF3'	$\nwarrow \nearrow \searrow$	$[J_s^2(\mathcal{J}_1 + \mathcal{J}_2 - 3\mathcal{J}_3 - E_M/3) - J_s H_{\parallel}]/3$
F3	$\nwarrow \nearrow \nwarrow \nearrow$	
F2	$\nwarrow \nearrow$	
C6	$\nwarrow \searrow \nwarrow \nearrow \searrow \nearrow$	

TABLE I. Stacking sequence of ferromagnetically ordered *ab*-planes along the *c*-axis for the phases found in the  $T = 2$  K magnetic anisotropic phase diagram in fig. 2. At low temperature the CEF forces the moments to lie in one of the four easy direction  $\langle 110 \rangle$  indicated by arrows. The external field forms an angle  $\theta$  with the  $(-1,1,0)$  ( $\nwarrow$ ) direction. The third column is the relevant part of the HFE per site, the term  $-J_s^2 \frac{\mathcal{J}_0}{2} - \frac{H^2}{8\pi}$  may be added to have the total HFE.  $H_{\parallel} = g\mu_B H \cos(\theta)$  is the projection of the field along the easy axis and all other symbols are explained in the text. We only give the HFE for the phases needed to compute the relations (4).

## FIGURES

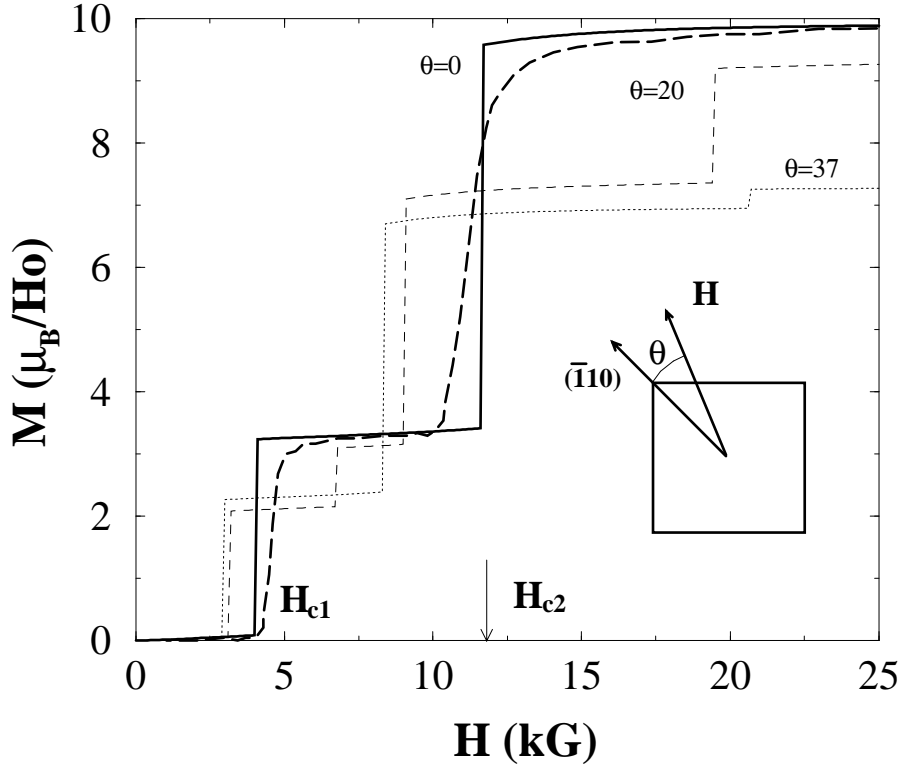


FIG. 1. Magnetisation vs. magnetic field for some representative angles  $\theta$  between the field and the closest  $\langle 110 \rangle$  direction. For  $\theta=0^\circ$  the thick dotted line represent experimental data taken from Canfield *et al* [12]. and the thick continuous line give results of our calculation. The two experimental parameters entering our model are the transition fields of the two metamagnetic transition  $H_{c1} = 4.1$  kG and  $H_{c2} = 11.1$  kG. This figure should be compared with fig. 1 (a) of [12]

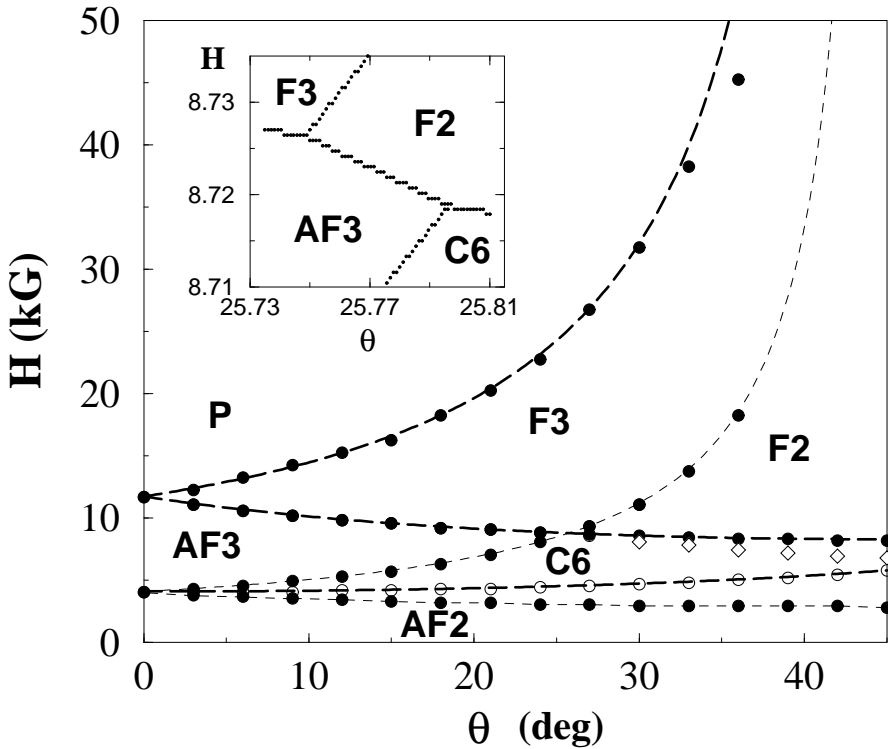


FIG. 2. Field vs. angle metamagnetic phase diagram for  $T = 2$  K. The filled dots are calculated within our model and indicate the phase transitions where a sensible jump in the magnetisation is seen ( $\Delta M > .2 \mu_B/H_0$ ). The thick dashed lines are given in [12] as the best fit of the experimental data. Their functional form is  $H_{c3}^0/\sin(45^\circ - \theta)$ ,  $H_{c2}^0/\cos(45^\circ - \theta)$  and  $H_{c1}^0/\cos\theta$ . The values we used for the proportionality constants are  $H_{c3}^0 = H_{c2}^0 = 8.4$  kG and  $H_{c1}^0 = 4.1$  kG. The two additional thin curves refer to the phase boundaries not yet observed in the experiments. Empty symbols refer to the stability of the  $AF3$  phase with respect to  $AF2$  (circles) and  $F2$  (diamonds). The apparent tetracritical point in the phase diagram is composed of two very close usual tricritical points (inset).